

RESEARCH ARTICLE

Histological, SEM and three-dimensional analysis of the midfacial SMAS – New morphological insights



T. Sandulescu, H. Buechner, D. Rauscher, E.A Naumova, W.-H Arnold*

Department of Biological and Material Sciences in Dentistry, School of Dentistry, Faculty of Health, Witten/Herdecke University, Germany

ARTICLE INFO

Article history:

Received 30 August 2018

Received in revised form 7 November 2018

Accepted 9 November 2018

Keywords:

SMAS

Superficial musculoaponeurotic system

Midface SMAS

Type IV SMAS

3D reconstruction

Histology

SEM

SMAS vascularization

ABSTRACT

Introduction: The superficial musculoaponeurotic system (SMAS) of the midface has a complex morphological architecture, and a multitude of controversial opinions exist regarding its in vitro appearance and clinical relevance. The aim of this study was to investigate the three-dimensional architecture of the midfacial SMAS.

Method: Histological and SEM analyses were performed on tissue blocks of the skin, subcutaneous tissue and mimic musculature of the midfacial region between the anterior parotid gland pole and lateral to the nasolabial fold and tissue blocks of the skin, subcutaneous tissue and parotid fascia. Blocks were collected postmortem from six formalin-fixed donor bodies. Serial histological sections were made, stained with Azan and digitized. Three-dimensional reconstructions and visualization of the tissue blocks were performed using AutoCAD.

Results: Two different SMAS architectures were found in the midfacial region: parotideal (type IV) and preparotideal (type I) SMAS. Type I SMAS showed three-dimensional interconnecting fibrous chambers embracing fat tissue lobules that cushioned the space between the skin and mimic musculature. Fibrous septa divided the mimic musculature surrounding the muscular bundles. Beneath the mimic muscular level, SMAS septa were oriented parallel to the muscular plane. Above the mimic muscular plane, SMAS septa were oriented perpendicularly, inserted into the skin. Type IV SMAS showed a parallel alignment of the fibrous septa to the skin level, anchoring the skin to the parotid fascia, presenting lymphatic nodes in the fat tissue compartments. The fat cells of the SMAS were enveloped in a fibrotic membrane at the border of the fibro-muscular septa. The SMAS blood supply comprised two subcutaneously epimuscularly spreading anastomosing vascular systems.

Conclusions: Midfacial SMAS represents a functional unit with physical and immunological tasks appearing in two different morphological architecture types. A well-defined nomenclature is needed to prevent controversy.

© 2018 The Author(s). Published by Elsevier GmbH. This is an open access article under the CC BY-NC-ND license (<http://creativecommons.org/licenses/by-nc-nd/4.0/>).

1. Introduction

The facial soft tissue anatomy, one of the most complex areas of the human body, has received intensive attention during the last decade as procedures of facial rejuvenation are being performed with increasing frequency and in numerous varieties (Cotofana et al., 2016; Khan and Bagheri, 2014). Since the description of the buccal fat pad by Bichat in 1801, a multitude of fibrous and fibro-muscular tissues dividing the facial fat in interacting compartments have been described (Cotofana et al., 2016, 2015; Kruglikov et al., 2016; Sandulescu et al., 2018a; Sykes et al., 2015; Weitgasser

et al., 2015). One accepted anatomical morphological model for the facial soft tissue is the layered concept, which is summarized by the acronym SCALP: S=skin (layer 1), C=connective tissue, here subcutaneous fat layer (layer 2), A=aponeurosis also musculoaponeurotic layer (layer 3), L=loose connective tissue, also areolar connective tissue (layer 4) and P=periosteum also deep fascia (layer 5) (Cotofana et al., 2016, 2015, 2014). Macroscopically, the subcutaneous fat layer (layer 2) occurs between the skin and the musculoaponeurotic system and is divided by fibrous septa into fatty tissue compartments (Gassner et al., 2008; Gierloff et al., 2012a; Gierloff et al., 2012b; Pilsl and Anderhuber, 2010a, 2010b). The superficial musculoaponeurotic system (SMAS), representing layer 3, connects the mimic musculature to the skin and has different regional morphological architectures (Ghassemi et al., 2003; Sandulescu et al., 2018a, 2018b). According to the histological anal-

* Corresponding author at: Department of Biological and Material Sciences in Dentistry, Alfred Herrhausenstrasse 44, 58455 Witten, Germany.

E-mail address: Wolfgang.Arndt@uni-wh.de (W.-H. Arnold).

ysis of Ghassemi et al., 2003, the nomenclature of type I SMAS and type II SMAS have been proposed: type I SMAS consists of fibrous septa connecting the mimic musculature to the skin and covering the skin lateral to the nasolabial fold, and type II SMAS shows a dense fibrous meshwork that is embedded with fat tissue that lies medial to the nasolabial fold. Although the SMAS concept is accepted in daily clinical practice, the lack of a precise definition has led to controversies concerning morphological composition and topographical expansion (De la Cuadra-Blanco et al., 2013; Ghassemi et al., 2003; Levet, 2004; Whitney and Zito, 2018). Additionally, the morphological variety of the SMAS morphology and composition has sustained this controversy in the literature (Broughton and Fyfe, 2013). Although macroscopic dissections after dye instillation into the different compartments and a three-dimensional imaging investigation described the compartmentation of the subcutaneous fat layer into two layers (layer 2 and 3) in the lateral midface, this has not yet been clearly demonstrated histologically (Broughton and Fyfe, 2013; Gassner et al., 2008; Pilsl and Anderhuber, 2010b).

Most clinical and experimental studies and descriptions agree about the existence of an SMAS structure in the cheek region lateral to the nasolabial fold (Cotofana et al., 2016, 2015; Fanous, 2006; Fanous et al., 2006; Ghassemi et al., 2003; Har-Shai et al., 1997; Khan and Bagheri, 2014; Macchi et al., 2010; Mendelson and Wong, 2013; Mitz and Peyronie, 1976; Sandulescu et al., 2018b; Weitgasser et al., 2015; Wong and Mendelson, 2013). Experimental studies have postulated that the architecture lateral to the nasolabial fold is of type I SMAS (Ghassemi et al., 2003). Cheek SMAS (type I SMAS) consists of fibrous septa of collagen fibers connecting the mimic musculature to the skin, which envelops fat tissue compartments (Ghassemi et al., 2003; Sandulescu et al., 2018a, 2018b).

In daily practice, cheek SMAS is a challenging structure in face-lifting procedures (Khan and Bagheri, 2014). Although the SMAS morphology has been investigated intensively, complications remain in daily clinical practice, including skin necrosis after face-lifting procedures that negatively affects the outcome of the surgical intervention and patient satisfaction (Giordano et al., 2017). The face-lift skin flap vasculature is supplied by the facial and transverse facial arteries (Wolff et al., 2005). Nevertheless, little is known about the microcirculation of the SMAS (Schuster et al., 1995; Whetzel and Stevenson, 1997). Therefore, an understanding of its morphology and topographical expansion is strongly needed (Ghassemi et al., 2003; Sandulescu et al., 2018a, 2018b).

This study is a comprehensive histological and architectural investigation of the lateral midface region (Mendelson and Jacobson, 2008) including the SMAS blood supply network and regional morphological differences.

The first hypothesis of this morphological investigation was that SMAS fibrous septa connect the mimic musculature to the skin and that their arrangement over the parotideal region is parallel to the skin level because of the lack of mimic musculature in this area; therefore, this area would be different than the SMAS type I architecture described.

In our previous study, we have shown that in the medial midface region lateral to the nasolabial fold, there is no strict histological discrimination between the subcutaneous fat layer (layer 2) and the musculoaponeurotic layer (layer 3). The SMAS fibrous septa of the medial midface expand through the subcutaneous fat layer, thus building a continuum with layer 2 and inserting into the skin (Sandulescu et al., 2018a, 2018b). There were no histological signs of a subcutaneous fat compartment.

Therefore, the second hypothesis of this study was that, in analogy to the results of our previous investigation, the subcutaneous fat layer (layer 2) of the lateral midface belongs to the SMAS (layer 3).

Table 1

Descriptive analysis of the body donor facial index, facial morphology, gender and age.

Donor body	Gender	Age	Facial index	Face morphology
1	Female	80 y	84.2	Euryprosopic
2	Female	80 y	80.4	Euryprosopic
3	Female	73 y	78.3	Hypereuryprosopic
4	Male	61 y	88.4	Mesoprosopic
5	Male	80 y	93.6	Leptoprosopic
6	Male	62 y	72.1	Hypereuryprosopic



Fig. 1. Donor side for the histological and for the SEM analysis (black ovals). The blue line topographically marks the border between the parotideal and prepartotideal regions. The red line marks the nasolabial fold. Modified from Radlanski and Wesker, (Radlanski, 2012) with the kind permission of Quintessence. (For interpretation of this figure in colour in this figure legend, the reader is referred to the web version of this article.)

2. Methods

The histomorphological investigation was performed on donor bodies, which were provided by the Department of Anatomy II, Friedrich-Alexander-Universität Erlangen-Nürnberg; these were official testamentary donations of volunteers to the Department for the anatomical student course for medical and dental students and for medical research purposes. The study was carried out according to the regulations of the WMA Declaration of Helsinki in its present form from 2013.

Full graft tissue blocks of the skin, SMAS and mimic musculature of the midfacial region (parotideal and prepartotideal regions) were collected postmortem from six (three male and three female) formalin-fixed donor bodies (Table 1). The facial index of each donor body was measured on en face photos, and the face morphological type was determined. The donor sites showed no visible scars or tissue damage, and the medical histories revealed no facial surgical interventions or radiation of the head and neck area. HIV infections and AIDS were not mentioned in the medical histories.

2.1. Histological analysis

After fixation in 4.5% formaldehyde, the tissue blocks taken from the parotideal and prepartotideal regions (Fig. 1) were embedded in paraffin, and serial histological sections in the vertical plane were

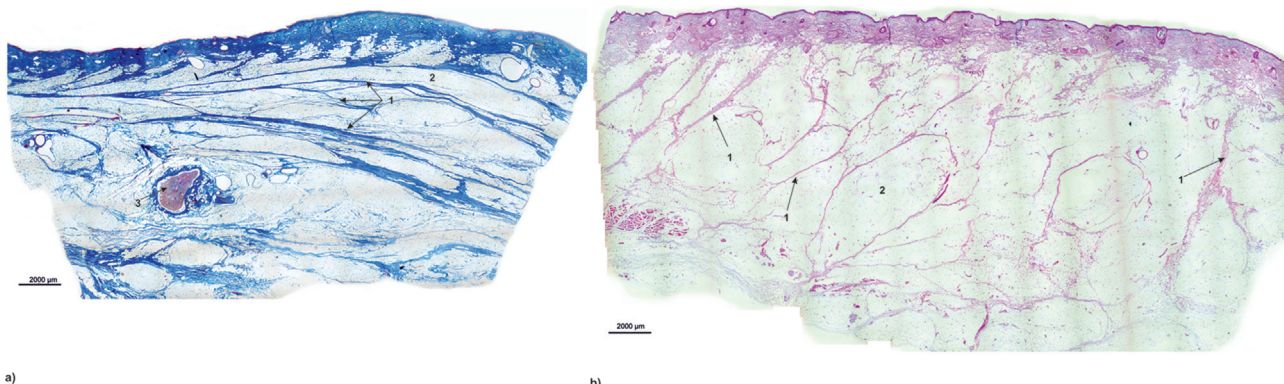


Fig. 2. Overview micrograph of histological sections. (a) Parotideal area; (b) preparotideal area. 1 = fibrous septa; 2 = SMAS fat compartment; 3 = lymph node.

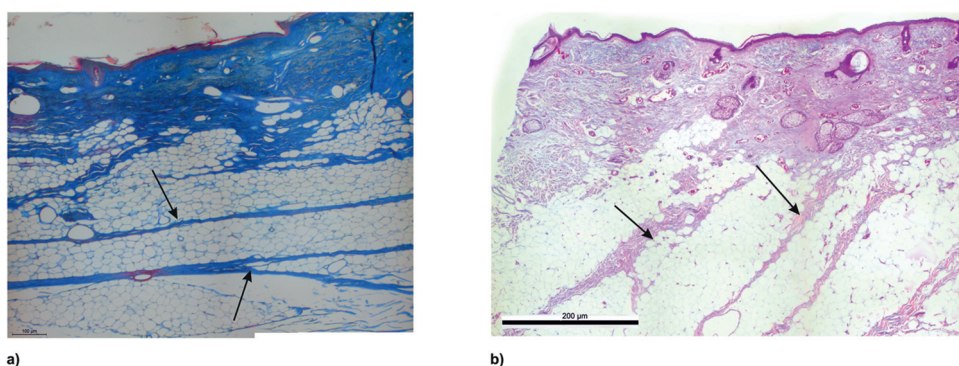


Fig. 3. Microphotograph of the SMAS. (a) Parotideal area; (b) preparotideal area. Arrows mark SMAS fibers.

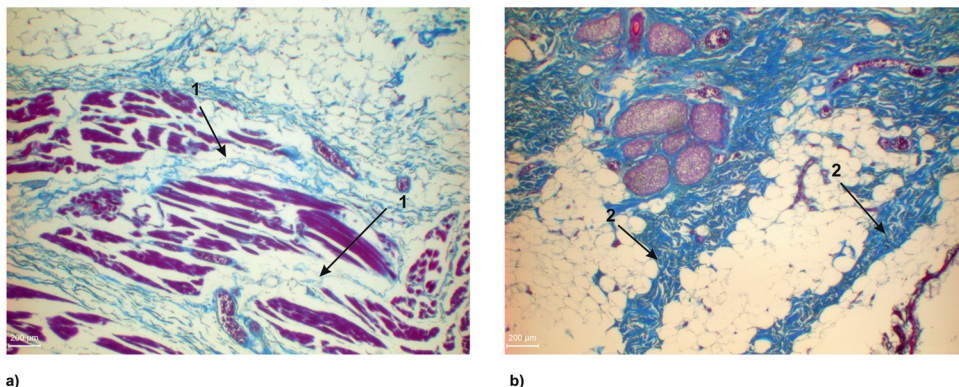


Fig. 4. Higher magnification of the preparotideal SMAS connecting the mimic musculature to the skin. (a) SMAS fibers (arrow 1) dividing the mimic musculature into muscular bundles; (b) docking area into the skin level with numerous irregularly arranged collagen fibers (arrow 2).

cut to a thickness of 5 µm. Every section was collected, and every 10th section was stained with Azan or Haematoxilin-Eosin (HE). Photomicrographs of the sections were taken with a Nikon D 7000 camera at a resolution of 12 megapixels. In addition, the sections were observed under a Leitz DMRB microscope (Leica, Wetzlar, Germany), and additional micrographs were taken.

2.2. SEM analysis

Two midfacial tissue blocks (parotideal and preparotideal regions) measuring 1 × 1 × 1 cm were post-fixed in 1% osmium tetroxide and dehydrated in graded alcohol. The specimens were critical-point dried and sputtered with gold-palladium using a Baltec sputter coater (Baltec, Belzers, Liechtenstein). The specimens were examined with a Zeiss Sigma VP scanning electron microscope

at 8 and 12 kV using the secondary electron detector (SE). Morphological analysis of the SMAS structures (fat cells, fibro-muscular septa and their skin insertions), mimic musculature and skin was performed to evaluate the tissue interaction and regional differences.

2.3. Three-dimensional reconstruction

3D reconstruction and rendering were performed using AutoCAD 2013 (Autodesk, Munich, Germany). Photographs of the histological sections were consecutively imported into AutoCAD 2013 and superimposed according to the best fit method. The outlines of the relevant structures were then digitized, each in separate layers. A total of 270 histological sections were digitized. Digitizing a single section required between 15 and 25 min depending on the

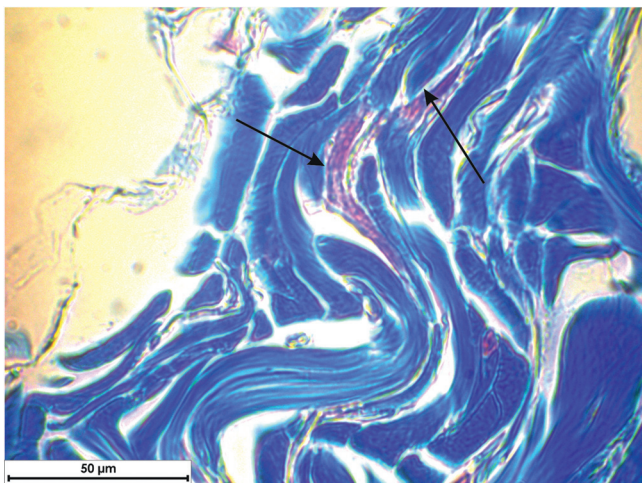


Fig. 5. Higher magnification of the muscular cells in the preparotideal SMAS fibrous septa. Arrows show muscular cells within the fibrous septa.

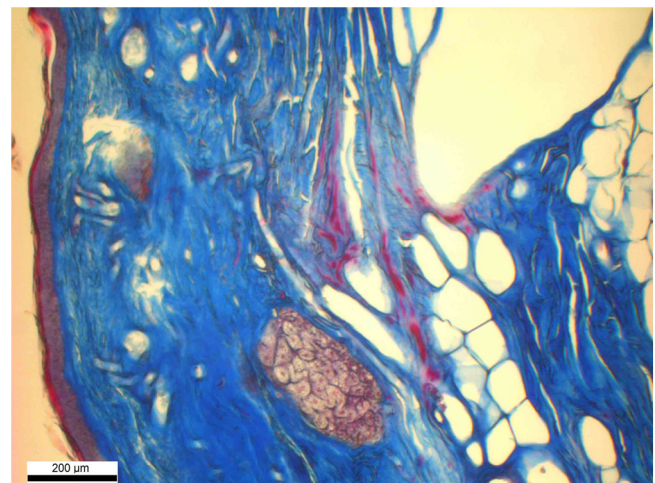


Fig. 7. Microphotograph of the parotideal SMAS showing the parallel alignment of the fibrous septa to the skin level. The arrow marks muscle cells in the fibrous cutaneous docking area.

complexity of the traced structures. A 3D meshwork wire-frame image was created from each structure. By freezing or thawing single structures (electronic dissection) (Machin et al., 1996), the three-dimensional architecture of the SMAS structures and their relations to the mimic musculature and the skin were demonstrated. The 3D wire-frame mesh was imported into 3D Studio (Autodesk, Munich, Germany), rendered into models and visualized from various angles.

3. Results

The macroscopical analysis of both parotideal and preparotideal histological sections of the tissue blocks revealed the existence of fibrous septa building fat compartments (Fig. 2). The preparotideal histological sections showed fibrous septa connections between the skin and the mimic muscles. Cutting artifacts occurred in the center of the histological series of the preparotideal region. There were no mimic muscles recognized in the parotideal histological sections. The overview showed vertical alignment of the fibrous septa to the skin level in the preparotideal sections (Fig. 2b) and parallel alignment of the fibrous septa to the skin in the parotideal (Fig. 2a) sections. Transverse-aligned small fibrous septa connected the parallel-aligned long fibrous connections between the skin and the mimic muscles.

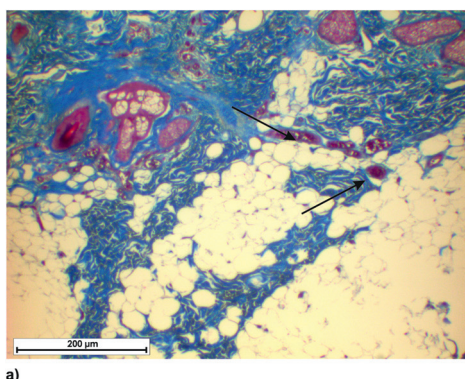


Fig. 6. Microphotograph of preparotideal SMAS blood vessels: (a) subcutaneous; (b) epimuscular. Arrows mark blood vessels.

3.1. Histological analysis

Morphologically, both parotideal and preparotideal SMAS contained fibro-muscular septa surrounding fat tissue compartments connecting the skin to a fibrous fascia and mimic musculature (Fig. 3).

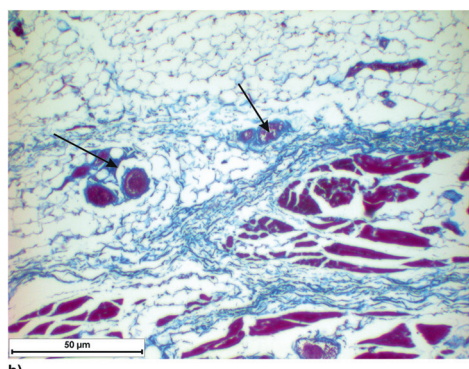
SMAS histological analysis revealed two regional different architectural types of the midfacial region:

- parotideal-type, comprising fibro-muscular septa with parallel alignment to the skin level (Fig. 3a), and
- preparotideal-type, showing fibro-muscular septa that were vertically aligned to the skin level (Fig. 3b).

Histologically, there were no delimitable fat tissue compartments between the skin (layer 1) and the SMAS (layer 3) in both the parotideal and preparotideal regions.

3.2. SMAS of the preparotideal region

Preparotideal SMAS contained vertical fibrous septa connecting the mimic musculature to the skin bordering fat tissue compartments (Fig. 4). Isolated muscle cells were found within the fibrous septa (Fig. 5). The fibrous septa perforated the mimic muscular plane, dividing it into muscular bundles. Beneath the mimic musculature, fibrous septa changed their orientation and were aligned parallel to the muscular plane. Beneath the mimic muscular plane,



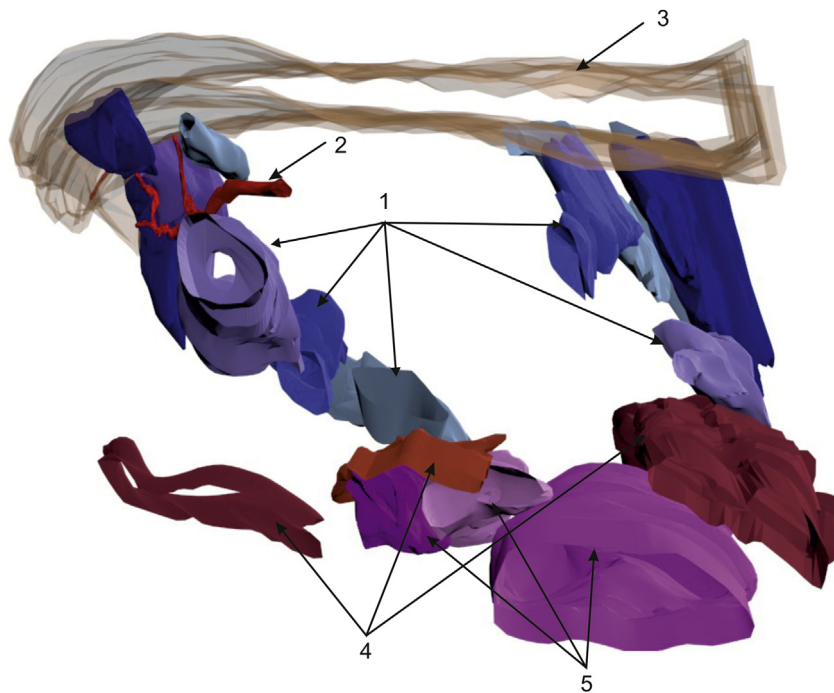


Fig. 8. 3D reconstruction of the preparotideal SMAS architecture showing the connection between the mimic musculature and the skin. 1 = skin; 2 = SMAS fat tissue compartments; 3 = the SMAS vascular system; 4 = mimetic muscle bundles; 5 = submuscular fat tissue compartments.

the fibrous septa enveloped fat tissue lobules that were smaller than the SMAS fat lobules.

Two vascular systems were recognized in the histological analysis. The SMAS blood supply system was divided into one vascular system spreading under the skin level and another spreading above the mimetic musculature plane (Fig. 6). No nervous structure was observed in the SMAS level.

The histological sections showed a multitude of cutting and staining artifacts in the central region of the histological series.

3.3. SMAS of the parotideal region

SMAS fibrous septa of the parotideal region were aligned parallel to the skin level, showing transverse, short interconnecting fibrotic connections. Like the preparotideal region, isolated muscle cells were identified within the fibrous septa close to the skin level (Fig. 7). A lymphatic node was identified in the parotideal SMAS (Figs. 2 and 9). The parotideal SMAS was connected deeply to a fibrous fascia by fibrous connective tissue.

3.4. 3D-reconstructions

The digitalized reconstruction of the tissue blocks revealed that SMAS is a three-dimensional meshwork of fibrous septa connecting the mimetic musculature to the skin in the preparotideal region (Fig. 8). The parotideal SMAS showed parallel alignment of the fibrous septa, into which were inserted obliquely short fibers connecting septa into the skin and parotideal fascia (Fig. 9). The vascular supply of the lymphatic node was irrigated by the subcutaneous SMAS vascular system.

3.5. SEM analysis

The SMAS of the preparotideal and parotideal regions had similar morphological compositions with different architectural arrangements. The regions were constructed of differently arranged fibrous septa building fat tissue compartments.

3.6. SMAS of the preparotideal region

The preparotideal SMAS consists of fibrous septa that are vertically aligned to the skin level and embrace compartments of fat tissue. SEM analysis of the preparotideal tissue block showed that the SMAS vascularization comprised two supply systems lying subcutaneously and epimuscularly, which were connected by corkscrew-like vertically running anastomoses (Fig. 10a). SMAS septa inserted into the skin level by numerous irregularly arranged connective tissue fibers. Toward the skin level, the diameter of the fibers decreased (Fig. 11a).

3.7. SMAS of the parotideal region

Parotideal region SMAS comprised fibrous septa that were arranged parallel to the skin level and enveloped fat tissue compartments (Fig. 10b). The skin insertion appeared similar to that of the preparotideal region, with numerous irregularly arranged fibers with decreasing diameter toward the insertion level (Fig. 11b).

3.8. SMAS fat tissue compartments

Both preparotideal and parotideal fat compartments were enveloped by a thin fibrous membrane demarcating the border of the fibrous septa (Fig. 12). The fat cells in the compartment were connected to each other by connective tissue fibers.

4. Discussion

SMAS and the fat compartments of the face, including their interactions with the mimetic muscles, have been described in the literature with some controversy since their first description in 1976 (Broughton and Fyfe, 2013; Cotofana et al., 2014; Ghassemi et al., 2003; Levet, 2004; Mitz and Peyronie, 1976; Rohrich and Pessa, 2007; Sandulescu et al., 2018a, 2018b). The lack of a precise definition of the structure of the SMAS and its vague differentiation from the fat compartments of the face have resulted in various interpre-

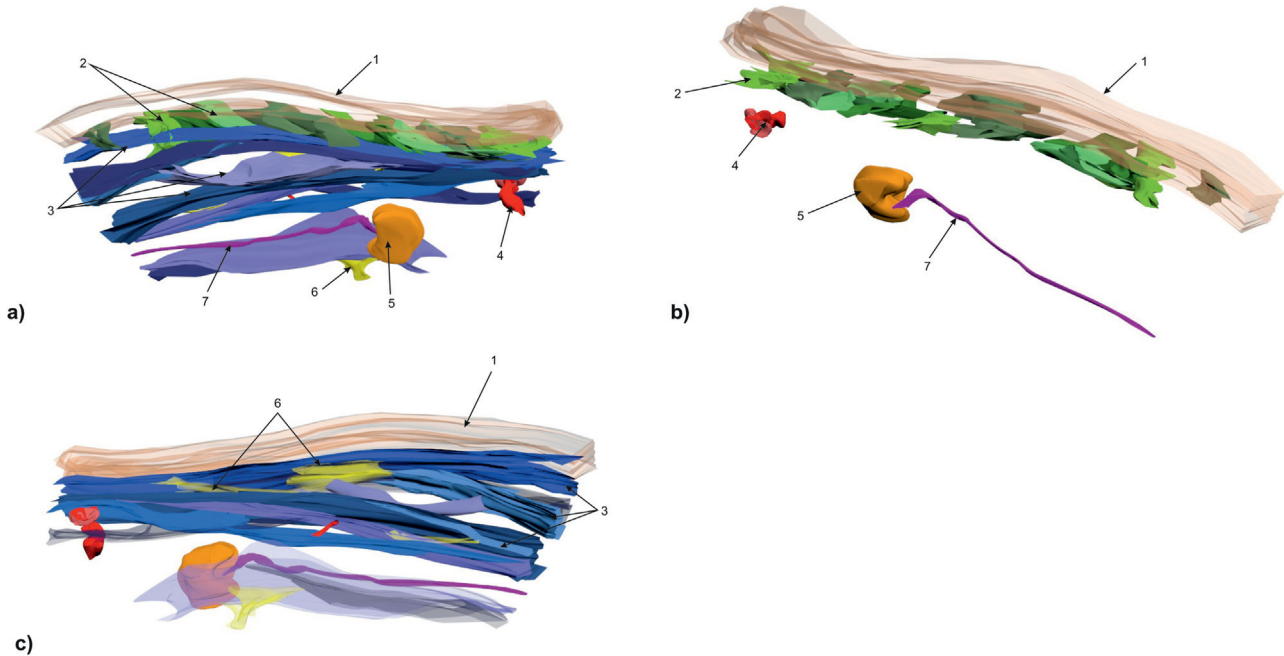


Fig. 9. 3D reconstruction of the parotideal SMAS architecture: (a), (b) region I lying subcutaneously with vertically aligned fibrous septa inserting into the skin; (c) region II with horizontally aligned fibrous septa with short interconnecting septa. 1 = skin; 2 = SMAS short, vertical, fibrous connective septa to the skin; 3 = SMAS horizontal fibrous septa; 4 = SMAS vascular irrigation system; 5 = SMAS lymphatic node; 6 = connecting fibers between horizontal fibers; 7 = lymphatic vessel.

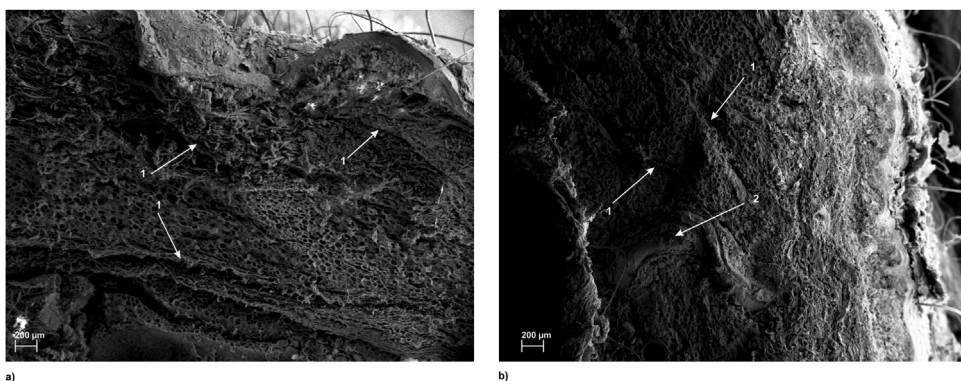


Fig. 10. (a) SEM micrograph of the preparotideal SMAS (b) parotideal SMAS architecture with fibrous septa inserting into the skin (arrows). 1 = SMAS fibers; 2 = anastomosis between the epimuscular and subcutaneous vascular systems.

tations and contradictory discussions (Broughton and Fyfe, 2013; Cotofana et al., 2016, 2015, 2014; Gierloff et al., 2012b; Macchi et al., 2010; Sandulescu et al., 2018b; Whitney and Zito, 2018).

In this study, SMAS histology and SEM morphology demonstrated regional differences in fibrous septa alignment between the preparotideal and parotideal regions. The 3D reconstruction demonstrated that the SMAS fibrous septa formed interconnecting spaces bolstered with fatty tissue. In conclusion, preparotideal and parotideal SMAS showed different fibrous septa arrangements. The two different SMAS architectures in the parotideal and preparotideal regions resulted in the conclusion that, following the description of Ghassemi et al. (2003), and Sandulescu et al. (2018a, 2018b), lateral to the nasolabial fold, there is, in addition to SMAS type I (Ghassemi et al., 2003; Sandulescu et al., 2018b), another, different parotideal SMAS morphological architecture that needs to be specified and that should be considered in the actual nomenclature. In former studies, three SMAS architecture types have been described: type I SMAS lateral to the nasolabial fold (Ghassemi et al., 2003; Sandulescu et al., 2018b), type II SMAS covering the area medial to the nasolabial fold (Ghassemi et al., 2003; Sandulescu

et al., 2018b), and type III SMAS covering the lower eyelid region cranial to the infraorbital fold (Sandulescu et al., 2018a). Therefore, a type IV SMAS is proposed for inclusion in the nomenclature for the parotideal region. Morphologically, type IV SMAS comprised a 3D network of fibrous septa with parallel alignment to the skin level, which created compartments bolstered with fatty tissue.

Anatomic macroscopic and three-dimensional imaging studies have investigated the shape of the facial fat compartments and their interaction with the bordering structures on non-fixed cadavers by injecting dye or colored Tandler gelatin into the different compartments followed by anatomic dissection (Pils and Anderhuber, 2010a, 2010b; Rohrich and Pessa, 2007) or by parallel anatomic macroscopic and three-dimensional imaging analysis (Gierloff et al., 2012a). In our study, we concentrated on the microscopic histological and SEM analysis of the SMAS and its microscopic architectural three-dimensional reconstruction, which was performed on histological serial sections from fixed tissue blocks. Due to the electronic dissection, the digitalization of the histologic structures and the 3D reconstruction of the tissue block allowed the individualized analysis of the interaction between the SMAS fibrous

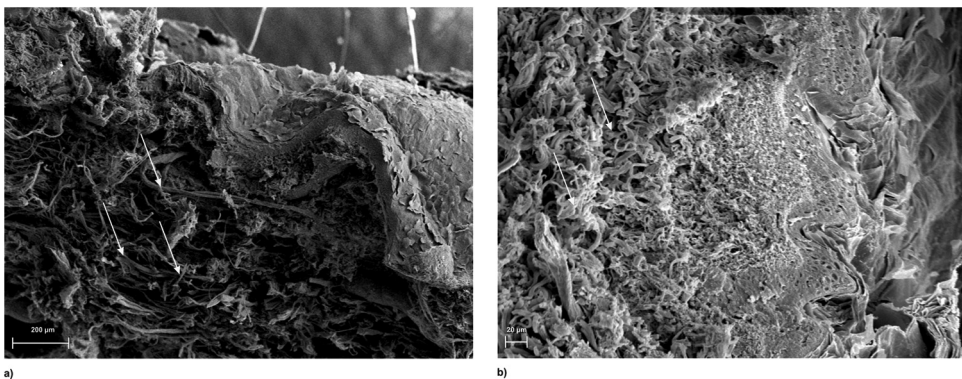


Fig. 11. (a) Higher magnification of the parotideal SMAS; (b) parotideal SMAS fibers inserting into the skin level.

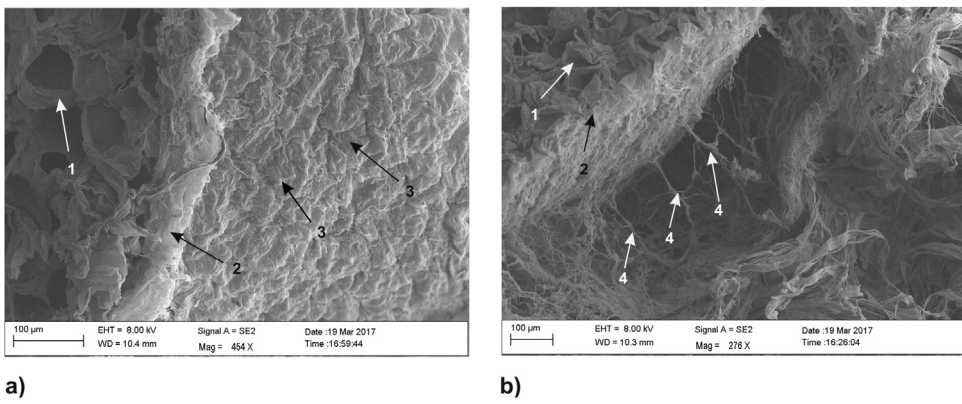


Fig. 12. (a) SEM micrograph of the thin fibrous membrane enveloping the fat compartments at the border with the SMAS fibrous septa. (b) Surface of the fibrous membrane enveloping the fat compartments and the anchoring fibers into the septum. 1 = fat cells; 2 = fibrous membrane surrounding the fat pads; 3 = imprints of the fat cells; anchoring fibers.

septa, the SMAS blood supply, the skin and the mimic muscles. This method has been described by Machin et al. (1996) for the reconstruction of histological serial sections of hard and soft tissues and was established for the morphological investigation of SMAS using formalin-fixed tissue blocks in our previous studies. By overlapping the histological and SEM analyses with the 3D reconstruction, we demonstrated that SMAS fibers create fibrous septa connecting the mimic muscles to the skin. Therefore, the mimic muscles do not have singular cutaneous insertions but interact extensively with the skin due to the SMAS interposition. Additionally, fibrous septa of parotideal SMAS were arranged parallel to the nasolabial fold, which might explain the formation of cutaneous wrinkles in the midface region parallel to the nasolabial fold.

In our opinion, the combination of the histological and SEM morphological analyses with the digitalization of the histological series and the 3D visualization of the tissue blocks was an appropriate method for understanding the morphological interactions among the facial soft tissues of the cheek.

4.1. Revisiting the anatomical facial layer concept

Our previous investigations showed that SMAS fibrous septa lateral to the nasolabial fold connect the mimic musculature to the skin (Sandulescu et al., 2018b). The conclusion was that SMAS fibrous septa are directly connected to the mimic musculature and to the skin. In this study, due to the lack of mimic musculature in the masticator/parotideal space, the lateral midface was divided (Mendelson and Jacobson, 2008) into parotideal and parotideal areas in a topographical analogy to the arrangement of the subcutaneous lateral-temporal and middle fat compart-

ments, respectively (Cotofana et al., 2015; Gierloff et al., 2012a, 2012b; Pisl and Anderhuber, 2010a, 2010b) to investigate the different arrangement of the SMAS fibrous septa and their interaction with the mimic musculature and the skin. In this study, parotideal and parotideal SMAS architectures showed different morphologies in terms of the fibrous septa alignment. In the parotideal region, SMAS fibrous septa were oriented parallel to the skin surface because of the lack of mimic musculature pointing towards the midcheek region and the nasolabial fold. In the parotideal region, SMAS architecture was similar to that demonstrated in our recent investigation and was lateral to the nasolabial fold (Sandulescu et al., 2018b). Although facial layers 2 and 3 have been demonstrated macroscopically (Cotofana et al., 2015), our histological serial section analysis and 3D reconstructions did not show two different layers in the midface region. In the SMAS of the parotideal region (layer 3), fibrous septa compartmented the subcutaneous fat layer (layer 2) without any boundaries. In the parotideal area, the subcutaneous fat layer was compartmentalized by fibrous SMAS septa that inserted into the overlying skin and into the underlying mimic muscles. As with the parotideal region, a strict differentiation of layers 2 and 3 was not possible in this area. Additionally, the subcutaneous muscular cells within the SMAS fibrous septa of the parotideal and parotideal regions support the hypothesis that the subcutaneous fibrous septa do not delimit the fat compartments but belong to the SMAS architecture, supporting the results of previous studies (Sandulescu et al., 2018a, 2018b). However, the existence of muscle cells within the SMAS fibers needs to be investigated further because the histological staining was nonspecific.

Within layer 2, the subcutaneous lateral-temporal and middle fat compartments have been macroscopically described after dye instillation followed by dissection and by three-dimensional imaging (Cotofana et al., 2015; Gierloff et al., 2012a; Pils and Anderhuber, 2010a, 2010b). In our study, we could not histologically confirm the existence of two different superficial fat compartments in the parotideal and preparotideal areas. In our opinion, the different fibrous septa alignment of the parotideal and preparotideal SMAS, together with the existence of the *septum subcutaneum parotideomassetericum*, might lead to distinct dye diffusion and distribution, thus explaining the macroscopic description of the two different subcutaneous fat compartments (layer 2) in this region (Cotofana et al., 2015; Gierloff et al., 2012a, 2012b; Pils and Anderhuber, 2010a, 2010b).

SEM analysis supported the histological results by revealing a fibrous connection between the fat cells in the compartments. On the surface, bordering the fibro-muscular septa, the fat compartments had a fibrous membrane. The membrane covering the fat compartments and its physiological function have not yet been described. According to the findings of this study, it is presumed that this membrane acts as an additional belt, thus improving the elasticity and stability of the fat compartments. According to the systematic fatty tissue classification of Sbarbati and colleagues, preparotideal and parotideal SMAS fatty tissue compartments can be characterized as type 2 structural white adipose tissue (sWAT) of the lobular subtype (Sbarbati et al., 2010), thus corresponding to the composition of the superficial fat compartments (Layer 2) (Kruglikov et al., 2016). Other than described by Kruglikov et al., the “Panniculus carnosus”, which separates the superficial from the deep fat compartments, could not be identified in our histological serial sections (Kruglikov et al., 2016). The results of previous studies have demonstrated that the “Panniculus carnosus” in the midfacial area does not always exist, due to morphological variability (Broughton and Fyfe, 2013; Cotofana et al., 2016, 2015; Weitgasser et al., 2015). Therefore, it was assumed that the absence of the “Panniculus carnosus” did not exclude the presence of the SMAS (layer 3). The fibrous connection between layers 2 and 3 in the preparotideal and parotideal areas, without strict discrimination between the two layers and the muscle cells in the SMAS fibrous septa, support our second hypothesis, which assumed that the subcutaneous fatty tissue is part of the SMAS.

4.2. Ontogenetically explanatory approach

Ontogenetically, the SMAS develops together with the superficial mimetic musculature, while the SMAS anlage maintains continuity with the platysma muscle (De la Cuadra-Blanco et al., 2013). However, the lack of a uniform facial architecture, especially for the superficial mimetic muscles, has not yet been clearly explained (Ghassemi et al., 2003; Levet, 2004). The different architecture and fibro-muscular septa alignment allowed the presumption that the SMAS develops ontogenetically together with the mimetic musculature, which drags it medially in the postero-anterior direction, thus supporting the embryological results of De la Cuadra-Blanco et al. (2013). Because of the lack of mimetic muscles superficial to the parotid gland, the parotideal SMAS is connected to the preparotideal mimetic muscles; therefore, its fibro-muscular septa are aligned horizontally to the skin level. These results might explain the histological observations made by Pils and Anderhuber, who described a similar arrangement of the parotideal fibrous tissue inserting into the *septum subcutaneum parotideomassetericum* (Pils and Anderhuber, 2010b). Nevertheless, the histological section of Pils and Anderhuber showed a similar parallel alignment of the fibrous septa to the skin level beyond the *septum subcutaneum parotideomassetericum* and the masseter muscle (Pils and Anderhuber, 2010b). Therefore, we assumed that the fibrous septa

aim toward the mimic muscles of the midfacial area, thus explaining the simultaneous development of the SMAS and mimic muscles (De la Cuadra-Blanco et al., 2013).

Histological and SEM analyses have revealed the vascular system of the parotideal and preparotideal SMAS units. The SMAS is supplied by two horizontally aligned vascular networks: the subcutaneous and epimuscular vascular networks. Corkscrew-like vessels connect the two vascular planes. These results contradict those of a previous investigation, in which the SMAS was described as a less-vascularized tissue (Schuster et al., 1995; Whetzel and Stevenson, 1997).

4.3. A proposed, new SMAS architectural nomenclature

According to our findings, the present midface SMAS nomenclature needs to be extended. Previous investigations described a singular type I SMAS morphological architecture lateral to the nasolabial fold and inferior to the infraorbital fold (Ghassemi et al., 2003; Sandulescu et al., 2018a, 2018b). The results of our study showed two different SMAS morphologies in the parotideal (type IV) and preparotideal (type I) regions. Considering the findings of Pils and Anderhuber (2010a, 2010b), it is assumed that the *septum subcutaneum parotideomassetericum* represents the border between type I and type IV SMAS. The preparotideal region was covered by type I SMAS, which was bordered by the nasolabial fold anteriorly, the infraorbital fold cranially and the *septum subcutaneum parotideomassetericum* laterally; these findings are similar to those obtained in a previous study (Macchi et al., 2010; Pils and Anderhuber, 2010b; Sandulescu et al., 2018a, 2018b). Additionally, type IV SMAS covered the parotideal area. Differently than the histological findings of Macchi et al. (2010), our histological and 3D reconstructions proved the existence of SMAS fibrous septa connecting the mimetic musculature to the skin in the preparotideal area (type I) (Macchi et al., 2010). The existence of type I and IV SMAS confirmed our hypothesis that the alignment of the fibrous septa is closely linked to the mimetic muscles.

4.4. Limitations

Our study was limited by the use of three male and three female formalin-fixed donor bodies. Therefore, gender-specific morphological differences could not be statistically analyzed. Another limitation was the use of body donors, the tissue of which is not always fixed properly due to the time span between death and fixation. The restricted regional and size of histological serial sections leave room for additional facial cartographic examination of the SMAS and its interaction with the overlying subcutaneous fat layer and to the underlying layers 4 and 5 beyond the boundaries of the model within the aim of this project.

In summary, the results of this study identify the lateral midface SMAS as an independent morphological and functional unit, such that the following specification of the histomorphological midface SMAS nomenclature is proposed:

Type I SMAS connects the mimetic muscles to the skin, forming a fibro-muscular meshwork of communicating compartments bolstered with fat tissue in the preparotideal region.

Type IV SMAS extends between the parotid fascia and the skin with a parallel alignment of the fibrous septa to the skin level.

5. Conclusions

The combination of histological and SEM morphological analyses with the digitalization of the histological serial sections and the 3D visualization of the tissue blocks is an appropriate method for understanding the morphological interactions among the soft tissues of the lateral midface.

The parotideal and preparotideal SMAS consists of connective, muscular, fat and lymphatic tissues that are directly connected with one another, representing a multifunctional unit undertaking physical and immunological tasks. The SMAS architecture of the midfacial area is subdivided into type I SMAS in the preparotideal region and type IV SMAS in the parotideal region. Based on the facial layer concept of anatomy, the subcutaneous fat layer (layer 2) and the SMAS (layer 3) form a singular functional unit with different morphological architectures.

SMAS fat compartments are strictly separated and can be distinguished from other facial fat compartments. SMAS fat compartments are enveloped at the junction of the fibrous septa by a fibrous membrane, whose function has not yet been investigated.

The reason for the different morphological architecture of the parotideal and preparotideal SMAS probably derives from their ontogenetical origins.

The supplying blood microsystem of the preparotideal and parotideal SMAS showed two horizontally aligned vascular networks spreading subcutaneously and epimuscularly, respectively, above the mimic muscular plane, connected by corkscrew-like vascular anastomoses.

The knowledge of the different morphological architectures of the cheek SMAS needs to be considered when performing surgical intervention in this area. Above all, there is a need for a uniform nomenclature for the SMAS morphology to prevent controversy.

Acknowledgement

We thank Susanne Haußmann for technical laboratory assistance in performing the serial histological sections and preparation of the tissue blocks for the SEM analysis.

References

- Broughton, M., Fyfe, G.M., 2013. The superficial musculoaponeurotic system of the face: a model explored. *Anat. Res. Int.* 2013, 794682.
- Cotofana, S., Fratila, A.A., Schenck, T.L., Redka-Swoboda, W., Zilinsky, I., Pavicic, T., 2016. The anatomy of the aging face: a review. *Facial Plast. Surg.* 32, 253–260.
- Cotofana, S., Schenck, T.L., Trevidic, P., Sykes, J., Massry, G.G., Liew, S., Graivier, M., Dayan, S., de Maio, M., Fitzgerald, R., Andrews, J.T., Remington, B.K., 2015. Mid-face: clinical anatomy and regional approaches with injectable fillers. *Plast. Reconstr. Surg.* 136, 219S–234S.
- Cotofana, S., Redka-Swoboda, W., Weitgasser, L., Schenck, T.L., 2014. The anatomy of the Superficial Musculo-Aponeurotic System (SMAS). *Kosmetische Medizin* 35, 224–233.
- De la Cuadra-Blanco, C., Peces-Pena, M.D., Carvallo-de Moraes, L.O., Herrera-Lara, M.E., Merida-Velasco, J.R., 2013. Development of the platysma muscle and the superficial musculoaponeurotic system (human specimens at 8–17 weeks of development). *Sci. World J.* 2013, 716962.
- Fanous, N., 2006. 'Optimum mobility' facelift. Part 1 – the theory. *Can. J. Plast. Surg.* 14, 67–73.
- Fanous, N., Karsan, N., Zakhary, K., Tawile, C., 2006. 'Optimum mobility' facelift. Part 2 – the technique. *Can. J. Plast. Surg.* 14, 75–87.
- Gassner, H.G., Rafii, A., Young, A., Murakami, C., Moe, K.S., Larrabee Jr., W.F., 2008. Surgical anatomy of the face: implications for modern face-lift techniques. *Arch. Facial. Plast. Surg.* 10, 9–19.
- Ghassemi, A., Prescher, A., Riediger, D., Axer, H., 2003. Anatomy of the SMAS revisited. *Aesthetic Plast. Surg.* 27, 258–264.
- Gierloff, M., Stohring, C., Buder, T., Gassling, V., Acil, Y., Wiltfang, J., 2012a. Aging changes of the midfacial fat compartments: a computed tomographic study. *Plast. Reconstr. Surg.* 129, 263–273.
- Gierloff, M., Stohring, C., Buder, T., Wiltfang, J., 2012b. The subcutaneous fat compartments in relation to aesthetically important facial folds and rhytides. *J. Plast. Reconstr. Aesthet. Surg.* 65, 1292–1297.
- Giordano, S., Koskivuo, I., Suominen, E., Verajankorva, E., 2017. Tissue sealants may reduce haematoma and complications in face-lifts: a meta-analysis of comparative studies. *J. Plast. Reconstr. Aesthet. Surg.* 70, 297–306.
- Har-Shai, Y., Bodner, S.R., Egozy-Golan, D., Lindenbaum, E.S., Ben-Izhak, O., Mitz, V., Hirshowitz, B., 1997. Viscoelastic properties of the superficial musculoaponeurotic system (SMAS): a microscopic and mechanical study. *Aesthetic Plast. Surg.* 21, 219–224.
- Khan, H.A., Bagheri, S., 2014. Surgical anatomy of the superficial musculo-aponeurotic system (SMAS). *Atlas Oral Maxillofac. Surg. Clin. N. Am.* 22, 9–15.
- Kruglikov, I., Trujillo, O., Kristen, Q., Isaac, K., Zorko, J., Fam, M., Okonkwo, K., Mian, A., Thanh, H., Koban, K., Sclafani, A.P., Steinke, H., Cotofana, S., 2016. The facial adipose tissue: a revision. *Facial Plast. Surg.* 32, 671–682.
- Levet, Y., 2004. A discussion of the article, anatomy of the SMAS revisited. *Aesthetic Plast. Surg.* 28, 123–124.
- Macchi, V., Tiengo, C., Porzionato, A., Stecco, C., Vigato, E., Parenti, A., Azzena, B., Weiglein, A., Mazzoleni, F., De Caro, R., 2010. Histotopographic study of the fibroadipose connective cheek system. *Cells Tissues Organs* 191, 47–56.
- Machin, G.A., Sperber, G.H., Ongaro, I., Murdoch, C., 1996. Computer graphic three-dimensional reconstruction of normal human embryo morphogenesis. *Anat. Embryol. (Berl.)* 194, 439–444.
- Mendelson, B.C., Jacobson, S.R., 2008. Surgical anatomy of the midcheek: facial layers, spaces, and the midcheek segments. *Clin. Plast. Surg.* 35, 395–404, discussion 393.
- Mendelson, B.C., Wong, C.H., 2013. Surgical anatomy of the middle premaxillary space and its application in sub-SMAS face lift surgery. *Plast. Reconstr. Surg.* 132, 57–64.
- Mitz, V., Peyronie, M., 1976. The superficial musculo-aponeurotic system (SMAS) in the parotid and cheek area. *Plast. Reconstr. Surg.* 58, 80–88.
- Pilsl, U., Anderhuber, F., 2010a. The chin and adjacent fat compartments. *Dermatol. Surg.* 36, 214–218.
- Pilsl, U., Anderhuber, F., 2010b. The septum subcutaneum parotideomassetericum. *Dermatol. Surg.* 36, 2005–2008.
- Radlanski, R.J., Wesker, K.H., 2012. *Das Gesicht. Quintessenz*, Berlin.
- Rohrich, R.J., Pessa, J.E., 2007. The fat compartments of the face: anatomy and clinical implications for cosmetic surgery. *Plast. Reconstr. Surg.* 119, 2219–2227, discussion 2228–2231.
- Sandulescu, T., Blaurock-Sandulescu, T., Buechner, H., Naumova, E.A., Arnold, W.H., 2018a. Three-dimensional reconstruction of the suborbicularis oculi fat and the infraorbital soft tissue. *JPRAS open* 16, 6–19.
- Sandulescu, T., Spilker, L., Rauscher, D., Naumova, E.A., Arnold, W.H., 2018b. Morphological analysis and three-dimensional reconstruction of the SMAS surrounding the nasolabial fold. *Ann. Anat.* 217, 111–117.
- Sbarbati, A., Accorsi, D., Benati, D., Marchetti, L., Orsini, G., Rigotti, G., Panettiere, P., 2010. Subcutaneous adipose tissue classification. *Eur. J. Histochem.* 54, e48.
- Schuster, R.H., Gamble, W.B., Hamra, S.T., Manson, P.N., 1995. A comparison of flap vascular anatomy in three rhytidectomy techniques. *Plast. Reconstr. Surg.* 95, 683–690.
- Sykes, J.M., Cotofana, S., Trevidic, P., Solish, N., Carruthers, J., Carruthers, A., Moradi, A., Swift, A., Massry, G.G., Lambros, V., Remington, B.K., 2015. Upper face: clinical anatomy and regional approaches with injectable fillers. *Plast. Reconstr. Surg.* 136, 204S–218S.
- Weitgasser, L., Cotofana, S., Schenck, T.L., Redka-Swoboda, W., 2015. The anatomy of the superficial musculo-aponeurotic system (SMAS). *Journal of Applied Aesthetics; Kosmetische Medizin* 5, 1–14.
- Whetzel, T.P., Stevenson, T.R., 1997. The contribution of the SMAS to the blood supply in the lateral face lift flap. *Plast. Reconstr. Surg.* 100, 1011–1018.
- Whitney, Z.B., Zito, P.M., 2018. Anatomy, skin (integument), fascias, superficial musculoaponeurotic system (SMAS) Fascia, StatPearls, Treasure Island (FL).
- Wolff, K.D., Bockmann, R., Nolte, D., Wysluch, A., Holzle, F., 2005. Limitations of blood supply to the skin flap in face lift surgery. *Mund-Kiefer- und Gesichtschirurgie: MKG* 9, 1–5.
- Wong, C.H., Mendelson, B., 2013. Facial soft-tissue spaces and retaining ligaments of the midcheek: defining the premaxillary space. *Plast. Reconstr. Surg.* 132, 49–56.